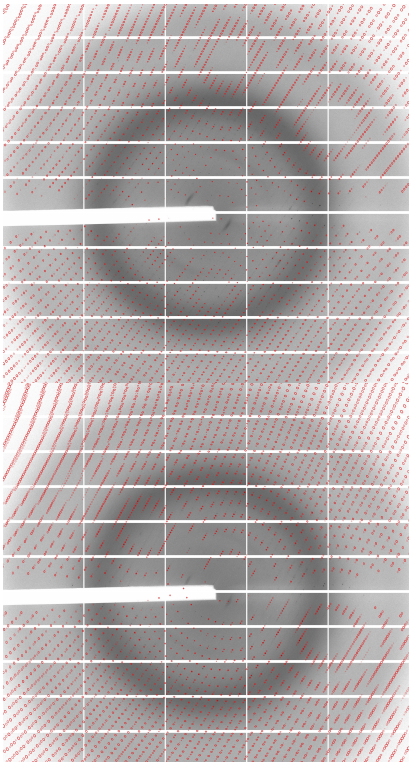

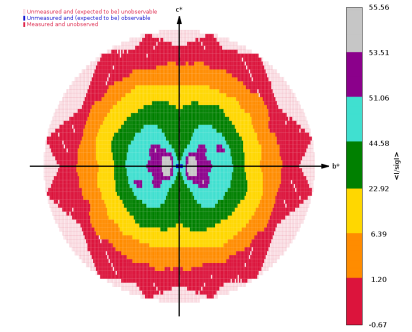

STARANISO local <I/sigI> H=0 plane

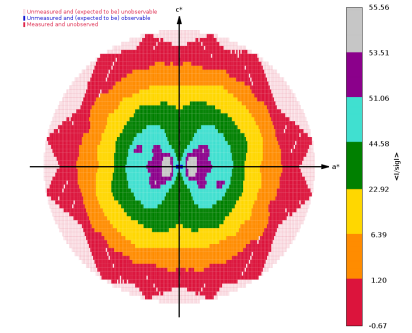

STARANISO local <I/sigI> K=0 plane

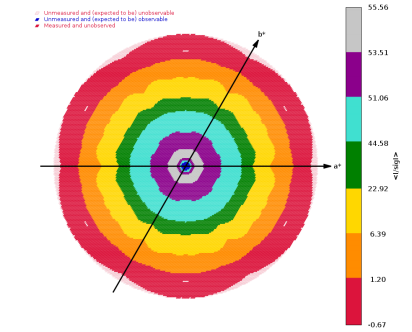

STARANISO local <I/sigI> L=0 plane

| | |
|---|---|
| autoPROC | 1.3.0 (20200318) |
| XDS | VERSION Jan 31, 2020 BUILT=20200131 |
| AIMLESS | Version 0.7.4 |
| STARANISO | Version 2.3.33 (11-Apr-2020) |
| CCP4 | Version 7.0.078 |
| Host | server8 |
| User | vonrhein (group = users) |
| Date | Mon Apr 20 10:01:13 CEST 2020 |
| autoPROC | /home/software/xtal/GPhL/20200420 |
| m4G4eg | m4G4eg_#####.cbf (54 images, 27°) |
| m4G4eg-2 | m4G4eg-2_#####.cbf (237 images, 118.5°) |
| m4G4eg-3 | m4G4eg-3_#####.cbf (175 images, 87.5°) |
| m4G4eg-4 | m4G4eg-4_#####.cbf (107 images, 53.5°) |
| m4G4eg-5 | m4G4eg-5_#####.cbf (66 images, 33°) |

## Anisotropic data analysis with STARANISO:

| | |
|---|---|
| **Spacegroup** | P3121 |
| **Cell parameters** | 168.5282 168.5282 51.9549 90.0 90.0 120.0 |
| **Wavelength [A]** | 0.97918 |
| **Diffraction limits [A]** | 1.970 1.970 1.909 |
| **Eigenvector-1** | 1.000 0.000 0.000 |
| **Eigenvector-2** | 0.000 1.000 0.000 |
| **Eigenvector-3** | 0.000 0.000 1.000 |
| **Direction-1** | 0.894 _a_* - 0.447 _b_* |
| **Direction-2** | _b_* |
| **Direction-3** | _c_* |

| | Overall | Inner Shell | Outer Shell |
|---|---|---|---|
| Low resolution limit | 48.946 | 48.946 | 2.009 |
| High resolution limit | 1.923 | 5.226 | 1.923 |
| | | | |
| Rmerge (all I+ & I-) | 0.160 | 0.062 | 6.190 |
| Rmeas (all I+ & I-) | 0.165 | 0.064 | 6.372 |
| Rpim (all I+ & I-) | 0.039 | 0.016 | 1.506 |
| Total number of observations | 1040750 | 56010 | 47339 |
| Total number unique | 58835 | 3336 | 2671 |
| Mean(I)/sd(I) | 16.5 | 49.2 | 1.3 |
| Completeness (spherical) | 91.5 | 100.0 | 34.1 |
| Completeness (ellipsoidal) | 95.2 | 100.0 | 49.3 |
| Multiplicity | 17.7 | 16.8 | 17.7 |
| CC(1/2) | 0.999 | 0.999 | 0.350 |
| | | | |
| Anomalous completeness (spherical) | 91.3 | 100.0 | 34.1 |
| Anomalous completeness (ellipsoidal) | 95.1 | 100.0 | 49.6 |
| Anomalous multiplicity | 9.1 | 9.0 | 9.0 |
| CC(ano) | -0.122 | -0.131 | 0.028 |
| \|DANO\|/sd(DANO) | 0.778 | 1.052 | 0.710 |

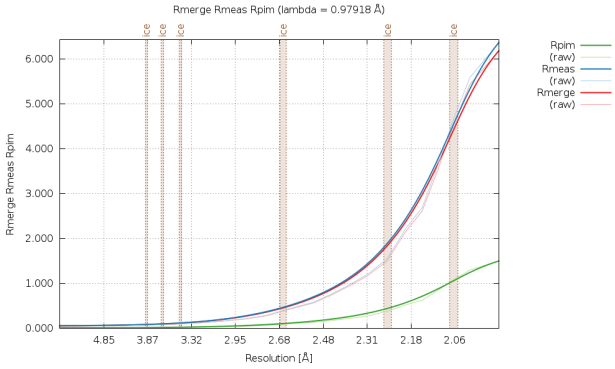


**Fig.1 :** R-values as a function of resolution (observations)

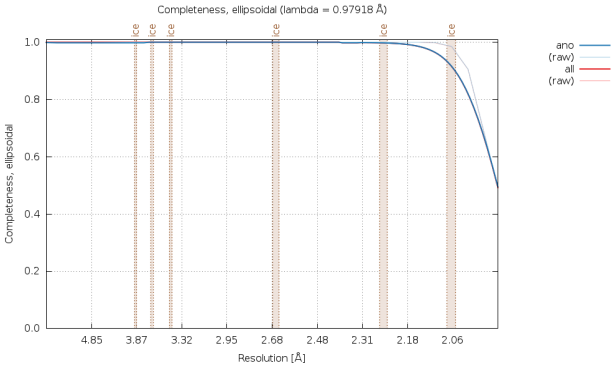


**Fig.2 :** Completeness (ellipsoidal) as a function of resolution (observations) - this is the relevant value here.

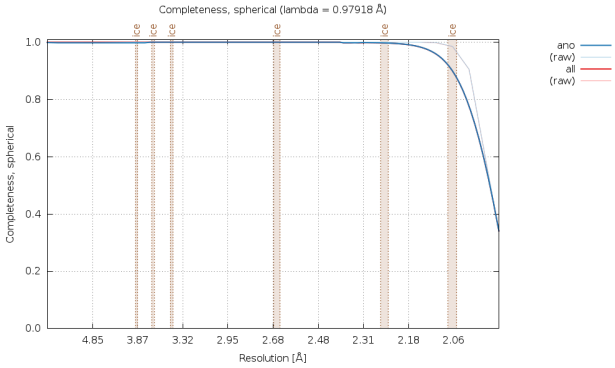


**Fig.3 :** Completeness (spherical) as a function of resolution (observations)

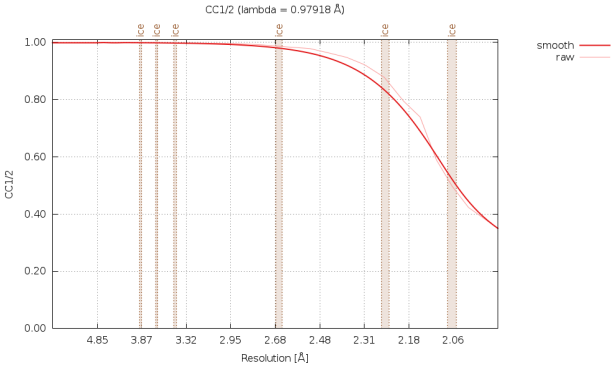


**Fig.4 :** CC1/2 as a function of resolution (observations)

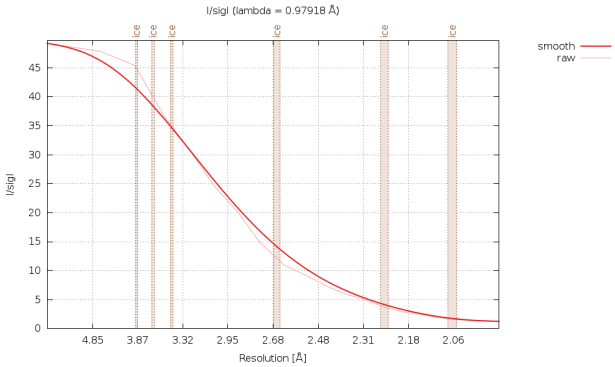


**Fig.5 :** I/sigI as a function of resolution (observations)

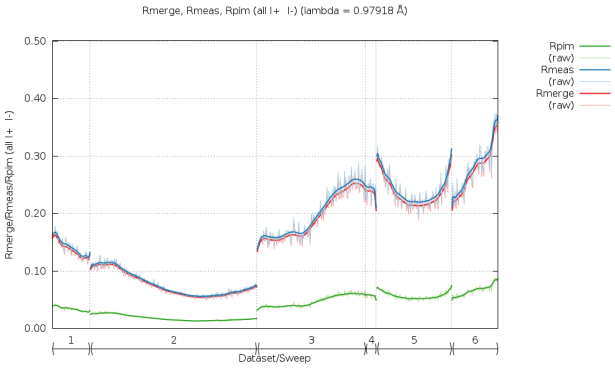


**Fig.6 :** R-values as a function of image number (observations)

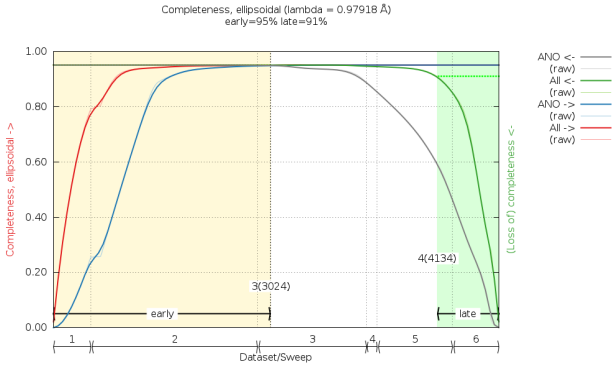


**Fig.7 :** Completeness (ellipsoidal) as a function of image number (observations) - this is the relevant value here.

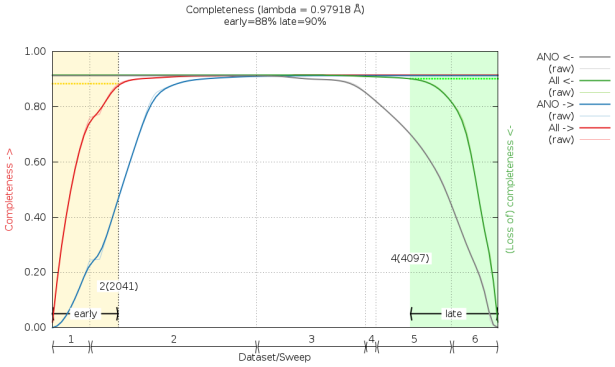


**Fig.8 :** Completeness (spherical) as a function of image number (observations)

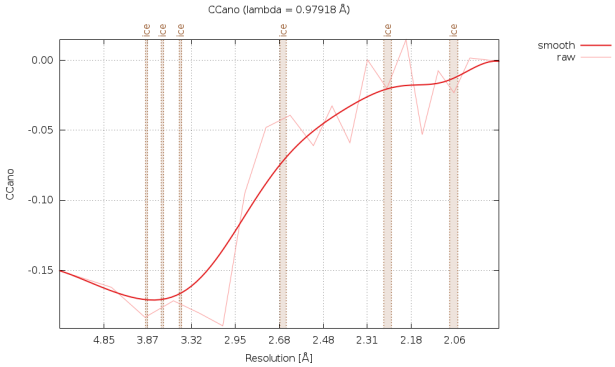


**Fig.9 :** CCano as a function of resolution (observations)

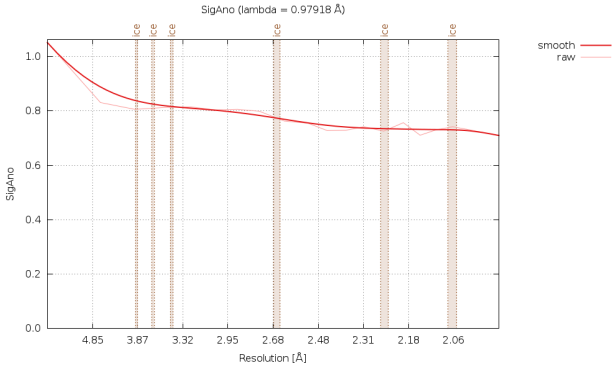


**Fig.10 :** SigAno as a function of resolution (observations)

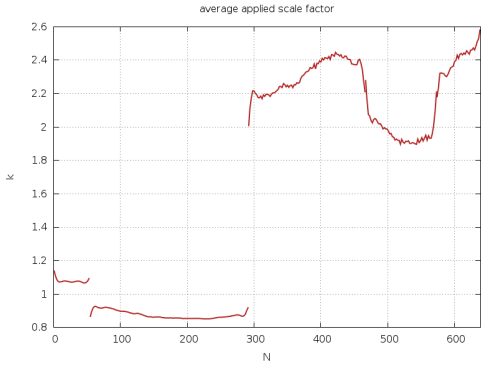


**Fig.11 :** Scale factor (isotropic AIMLESS scaling) as a function of image number (measurements)

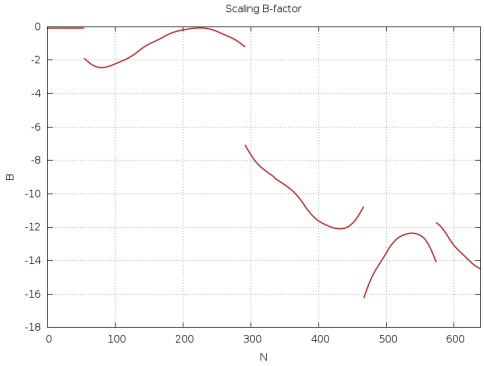


**Fig.12 :** Scaling B-factor (isotropic AIMLESS scaling) as a function of image number (measurements)

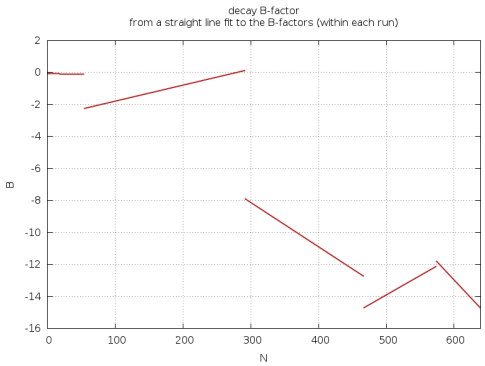


**Fig.13 :** Decay B-factor (isotropic AIMLESS scaling) as a function of image number (measurements)

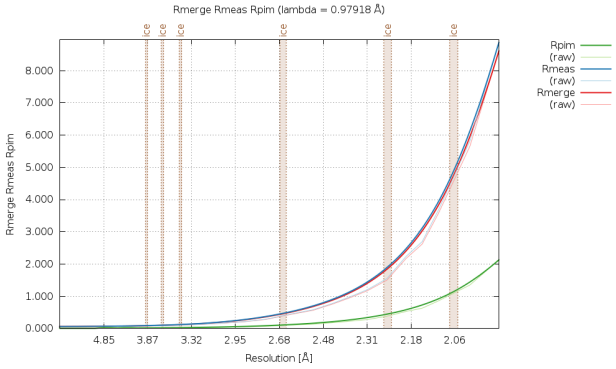


**Fig.14 :** R-values as a function of resolution (measurements)

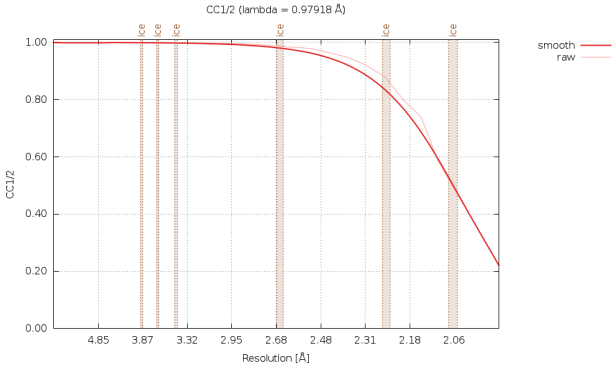


**Fig.15 :** CC1/2 as a function of resolution (measurements)

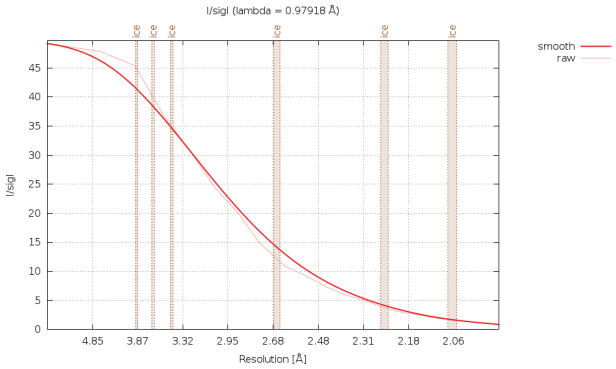


**Fig.16 :** I/sigI as a function of resolution (measurements)

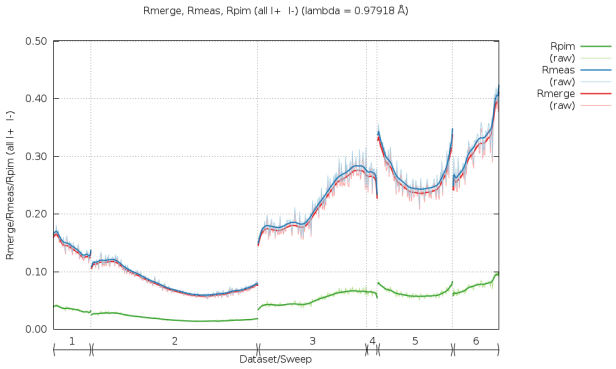


**Fig.17 :** R-values as a function of image number (measurements)

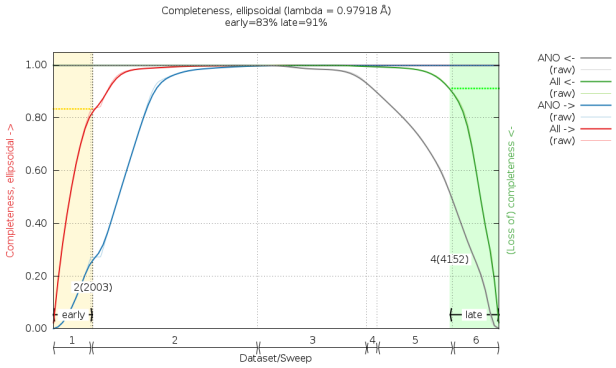


**Fig.18 :** Completeness (ellipsoidal) as a function of image number (measurements)

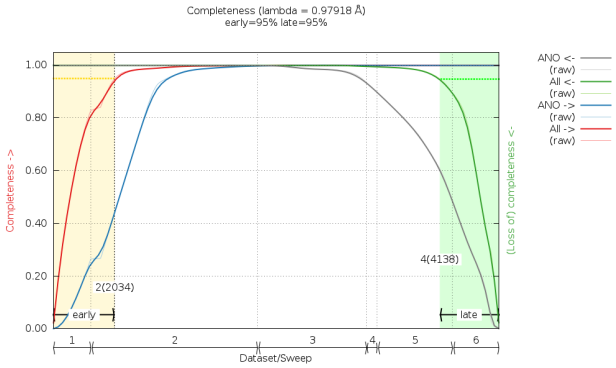


**Fig.19 :** Completeness (spherical) as a function of image number (measurements)

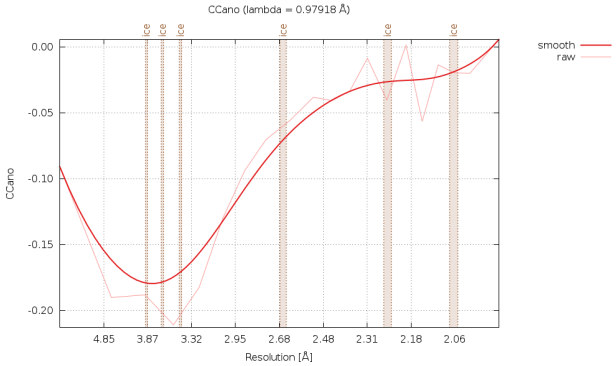


**Fig.20 :** CCano as a function of resolution (measurements)

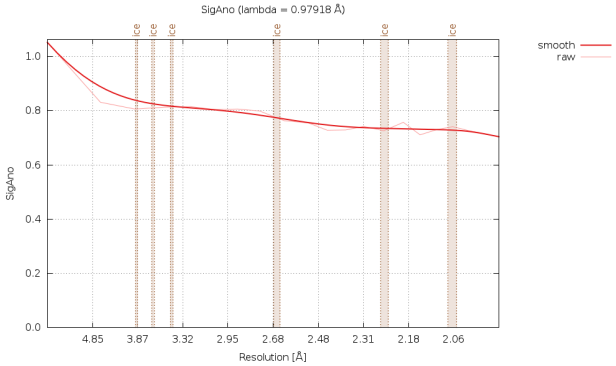


**Fig.21 :** SigAno as a function of resolution (measurements)

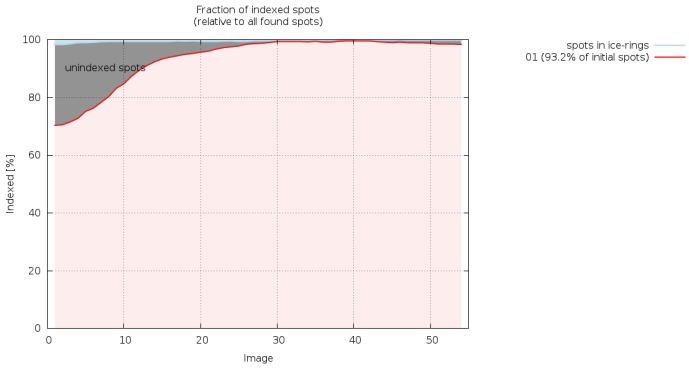


**Fig.22 :** (sweep m4G4eg) number of spots for each indexing solution as a function of image number

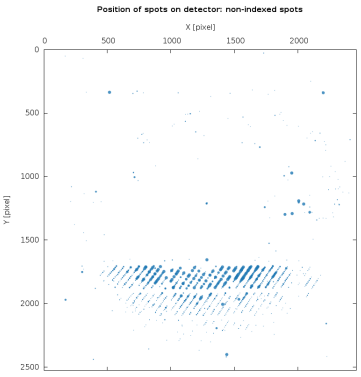


**Fig.23 :** (sweep m4G4eg) unindexed spots as a function of detector position

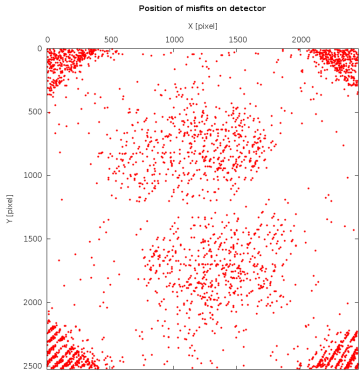


**Fig.24 :** (sweep m4G4eg) reflections classified as misfits (as a function of detector position)

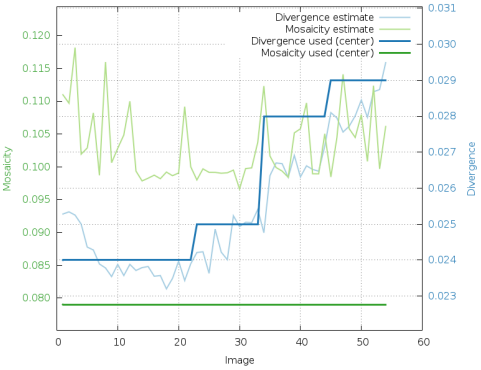


**Fig.25 :** (sweep m4G4eg) divergence and mosaicity (estimated and used) as a function of image number

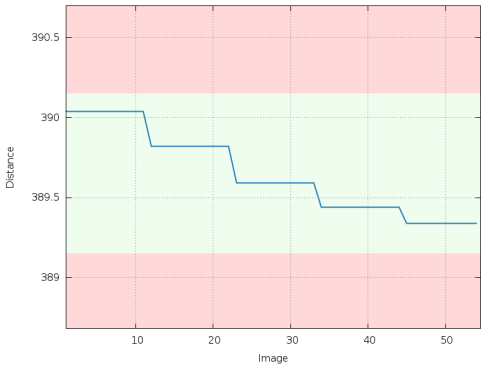


**Fig.26 :** (sweep m4G4eg) refined crystal-to-detector distance as a function of image number

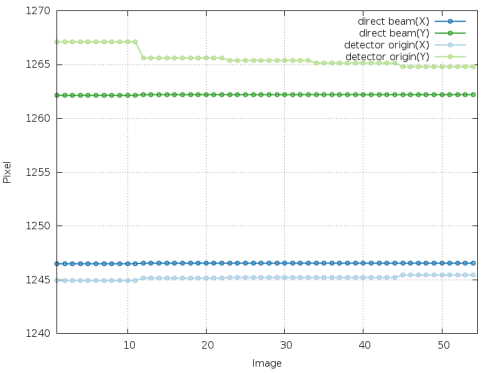


**Fig.27 :** (sweep m4G4eg) direct beam position and detector origin as a function of image number

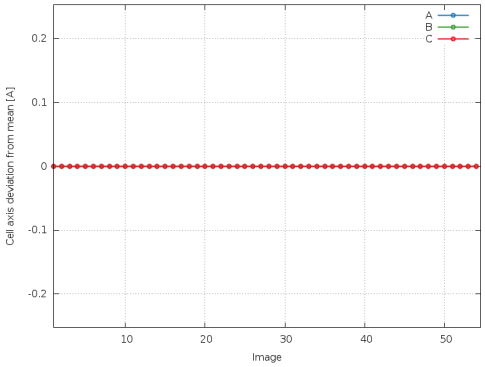


**Fig.28 :** (sweep m4G4eg) deviation of refined cell axes relative to their mean (as a function of image number)

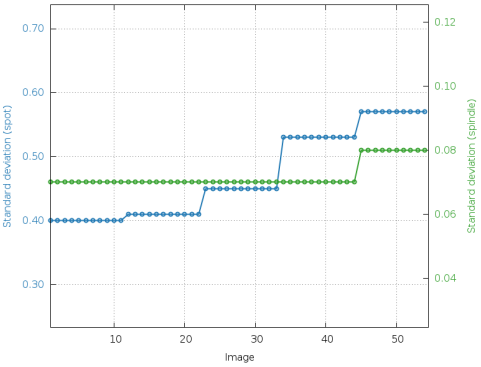


**Fig.29 :** (sweep m4G4eg) standard deviation (spot position and spindle) as a function of image number

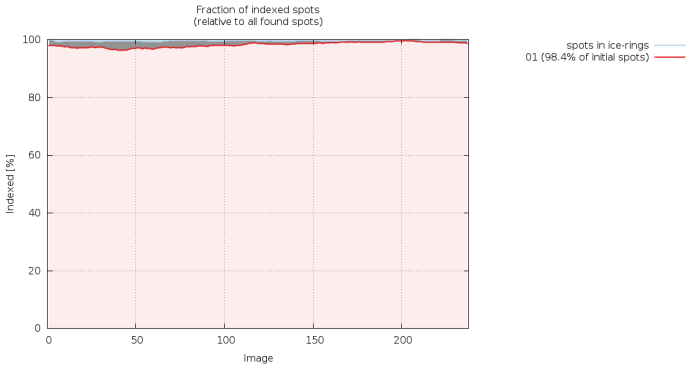


**Fig.30 :** (sweep m4G4eg-2) number of spots for each indexing solution as a function of image number

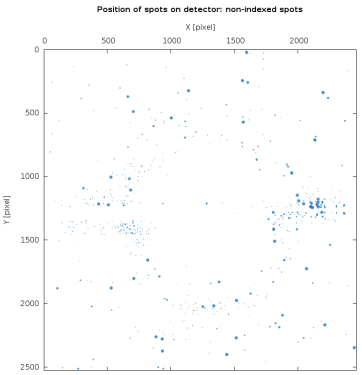


**Fig.31 :** (sweep m4G4eg-2) unindexed spots as a function of detector position

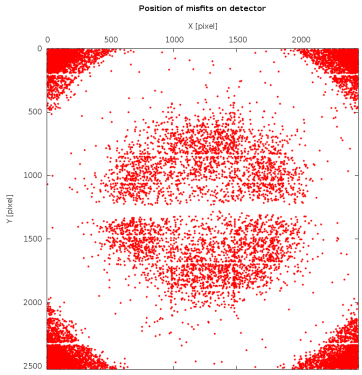


**Fig.32 :** (sweep m4G4eg-2) reflections classified as misfits (as a function of detector position)

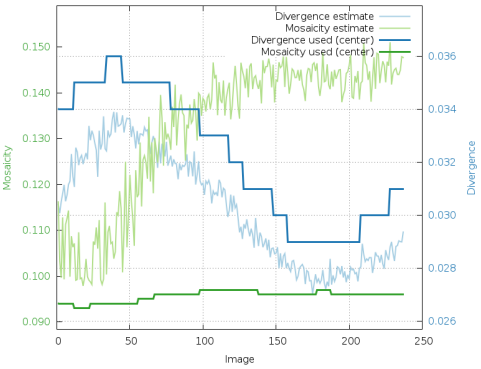


**Fig.33 :** (sweep m4G4eg-2) divergence and mosaicity (estimated and used) as a function of image number

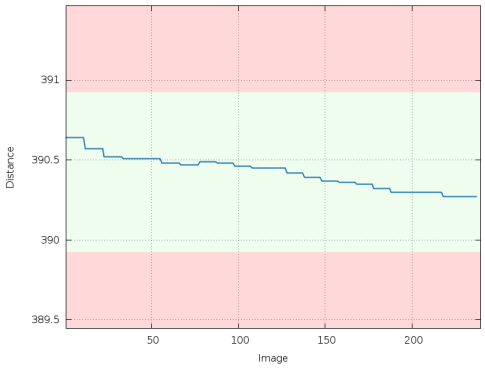


**Fig.34 :** (sweep m4G4eg-2) refined crystal-to-detector distance as a function of image number

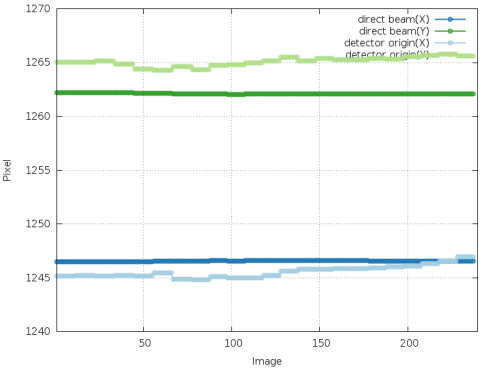


**Fig.35 :** (sweep m4G4eg-2) direct beam position and detector origin as a function of image number

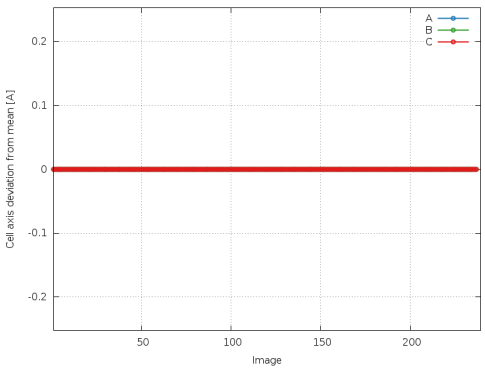


**Fig.36 :** (sweep m4G4eg-2) deviation of refined cell axes relative to their mean (as a function of image number)

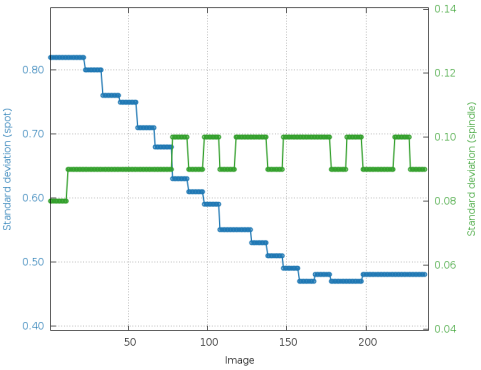


**Fig.37 :** (sweep m4G4eg-2) standard deviation (spot position and spindle) as a function of image number

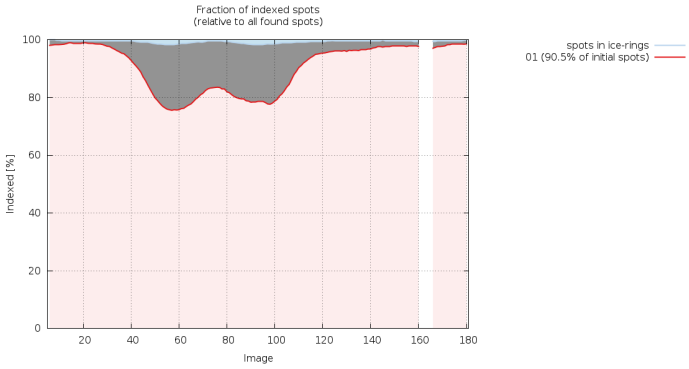


**Fig.38 :** (sweep m4G4eg-3) number of spots for each indexing solution as a function of image number

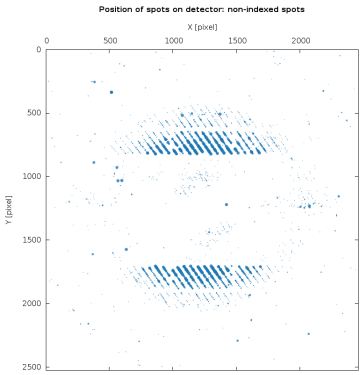


**Fig.39 :** (sweep m4G4eg-3) unindexed spots as a function of detector position

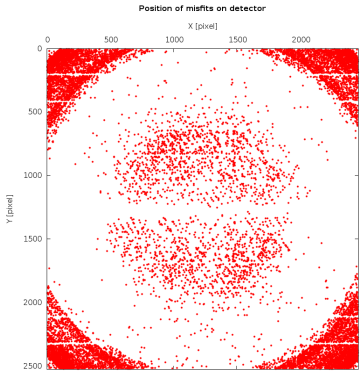


**Fig.40 :** (sweep m4G4eg-3) reflections classified as misfits (as a function of detector position)

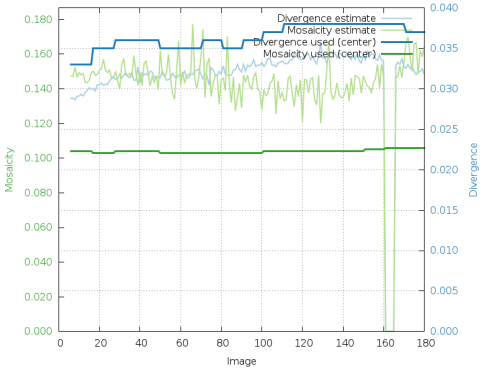


**Fig.41 :** (sweep m4G4eg-3) divergence and mosaicity (estimated and used) as a function of image number

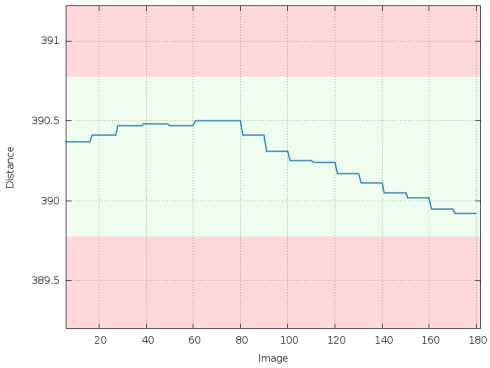


**Fig.42 :** (sweep m4G4eg-3) refined crystal-to-detector distance as a function of image number

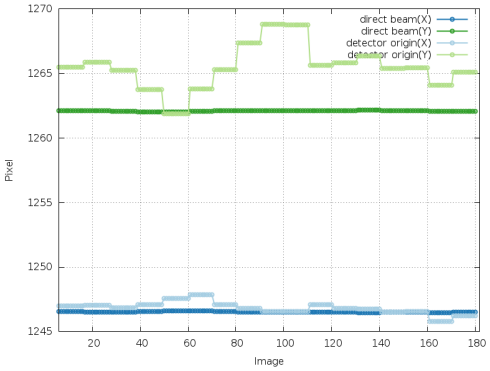


**Fig.43 :** (sweep m4G4eg-3) direct beam position and detector origin as a function of image number

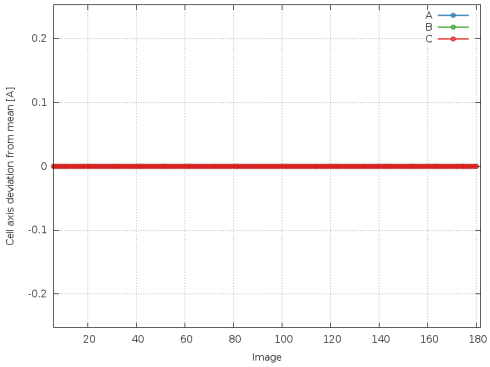


**Fig.44 :** (sweep m4G4eg-3) deviation of refined cell axes relative to their mean (as a function of image number)

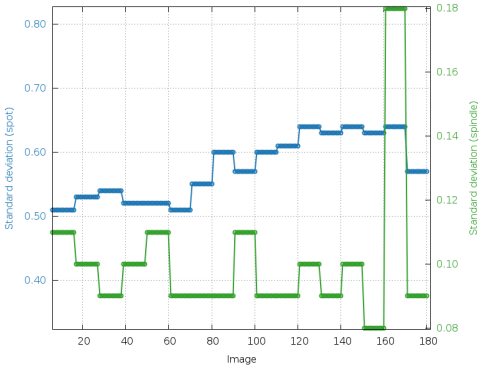


**Fig.45 :** (sweep m4G4eg-3) standard deviation (spot position and spindle) as a function of image number

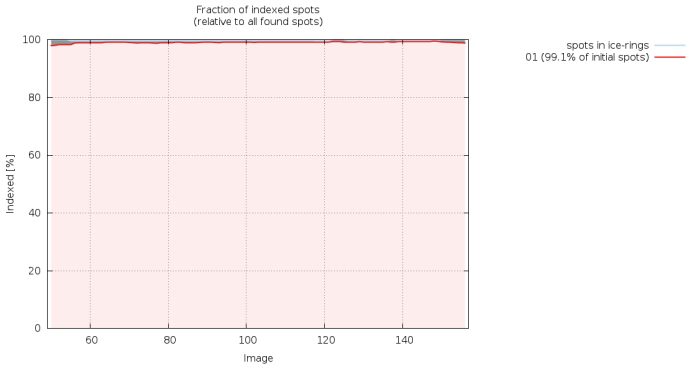


**Fig.46 :** (sweep m4G4eg-4) number of spots for each indexing solution as a function of image number

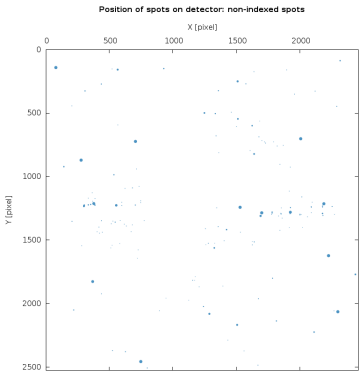


**Fig.47 :** (sweep m4G4eg-4) unindexed spots as a function of detector position

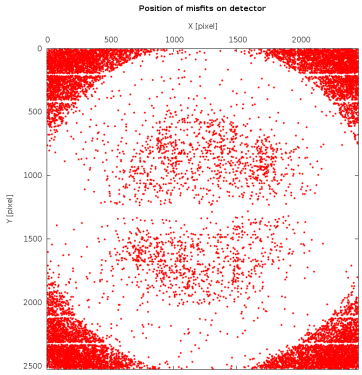


**Fig.48 :** (sweep m4G4eg-4) reflections classified as misfits (as a function of detector position)

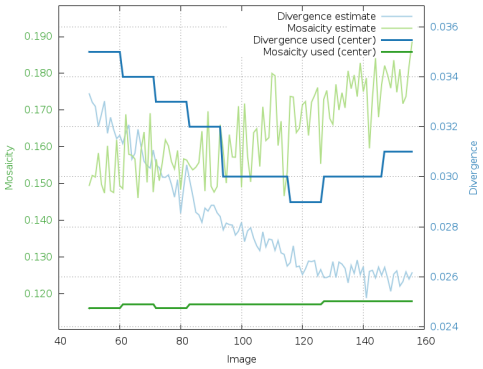


**Fig.49 :** (sweep m4G4eg-4) divergence and mosaicity (estimated and used) as a function of image number

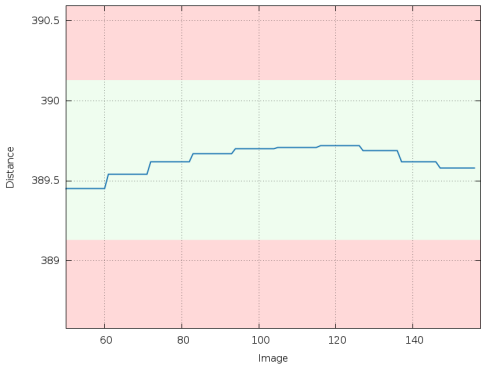


**Fig.50 :** (sweep m4G4eg-4) refined crystal-to-detector distance as a function of image number

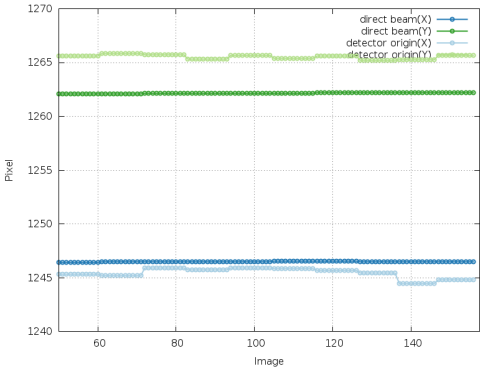


**Fig.51 :** (sweep m4G4eg-4) direct beam position and detector origin as a function of image number

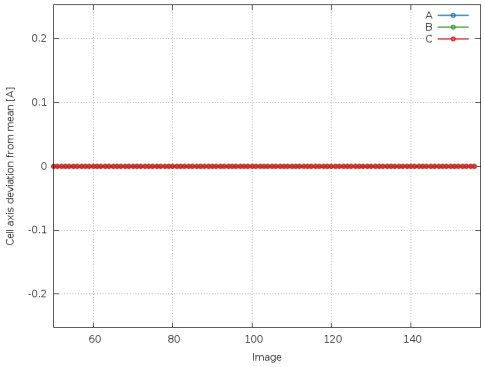


**Fig.52 :** (sweep m4G4eg-4) deviation of refined cell axes relative to their mean (as a function of image number)

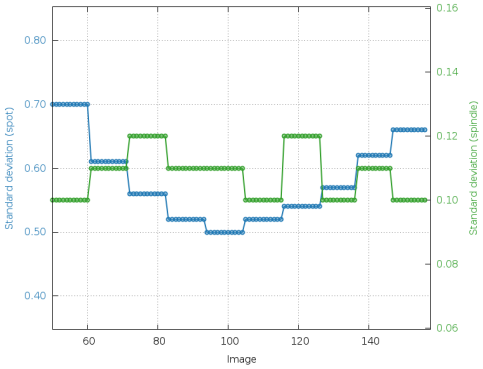


**Fig.53 :** (sweep m4G4eg-4) standard deviation (spot position and spindle) as a function of image number

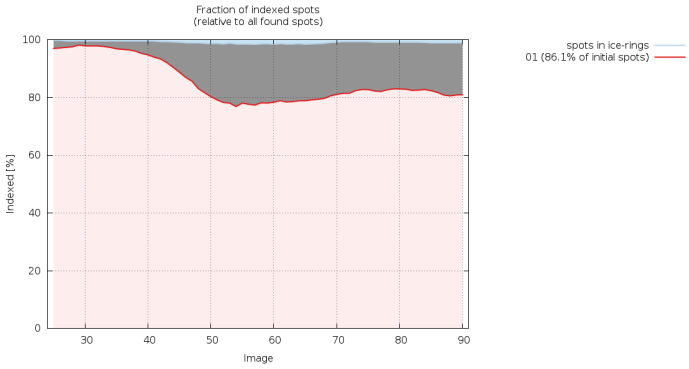


**Fig.54 :** (sweep m4G4eg-5) number of spots for each indexing solution as a function of image number

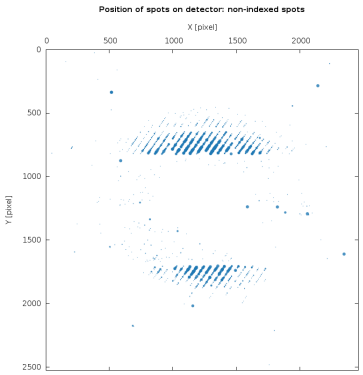


**Fig.55 :** (sweep m4G4eg-5) unindexed spots as a function of detector position

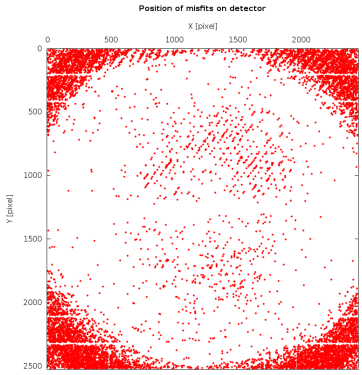


**Fig.56 :** (sweep m4G4eg-5) reflections classified as misfits (as a function of detector position)

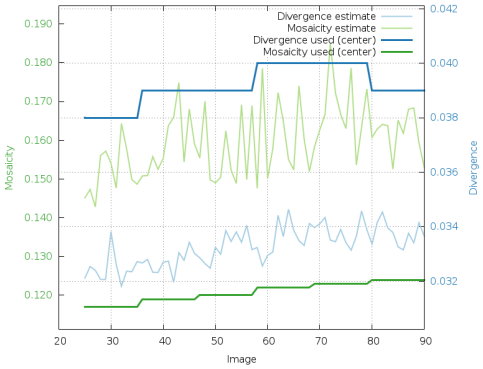


**Fig.57 :** (sweep m4G4eg-5) divergence and mosaicity (estimated and used) as a function of image number

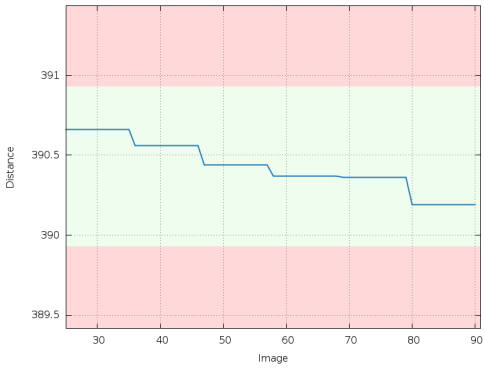


**Fig.58 :** (sweep m4G4eg-5) refined crystal-to-detector distance as a function of image number

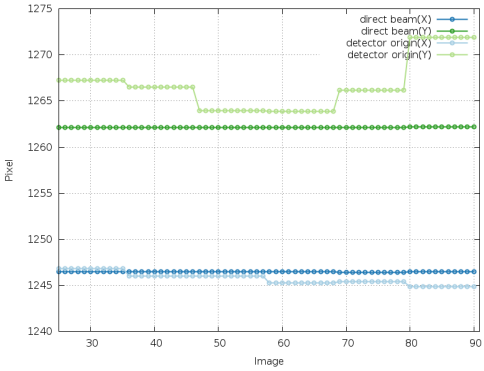


**Fig.59 :** (sweep m4G4eg-5) direct beam position and detector origin as a function of image number

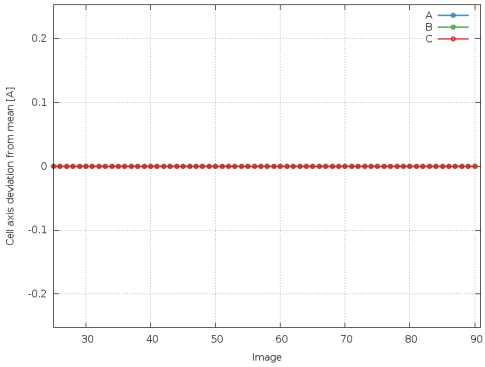


**Fig.60 :** (sweep m4G4eg-5) deviation of refined cell axes relative to their mean (as a function of image number)

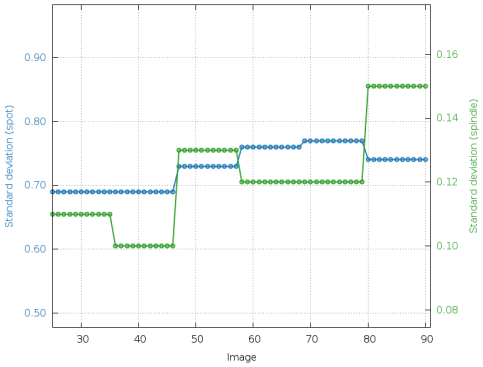


**Fig.61 :** (sweep m4G4eg-5) standard deviation (spot position and spindle) as a function of image number

| | |
|---|---|
| autoPROC | Vonrhein, C., Flensburg, C., Keller, P., Sharff, A., Smart, O., Paciorek, W., Womack, T. and Bricogne, G. (2011). Data processing and analysis with the autoPROC toolbox. Acta Cryst. D67, 293-302. |
| XDS | Kabsch, W. (2010). XDS. Acta Cryst. D66, 125-132. |
| POINTLESS | Evans, P.R. (2006). Scaling and assessment of data quality, Acta Cryst. D62, 72-82. |
| AIMLESS | Evans, P.R. and Murshudov, G.N. (2013). How good are my data and what is the resolution?, Acta Cryst. D69, 1204-1214. |
| CCP4 | Winn, M.D., Ballard, C.C., Cowtan, K.D. Dodson, E.J., Emsley, P., Evans, P.R., Keegan, R.M., Krissinel, E.B., Leslie, A.G.W., McCoy, A., McNicholas, S.J., Murshudov, G.N., Pannu, N.S., Potterton, E.A., Powell, H.R., Read, R.J., Vagin, A. and Wilson, K.S. (2011). Overview of the CCP4 suite and current developments, Acta. Cryst. D67, 235-242. |
| STARANISO | Tickle, I.J., Flensburg, C., Keller, P., Paciorek, W., Sharff, A., Vonrhein, C., and Bricogne, G. (2020). STARANISO. Cambridge, United Kingdom: Global Phasing Ltd. |